Semi-automated Tracking and Continuous Monitoring of Inferior Vena Cava Diameter in Simulated and Experimental Ultrasound Imaging.

(Article begins on next page)

01 May 2024

UNIVERSITÀ DEGLI STUDI DI TORINO

http://dx.doi.org/10.1016/j.ultrasmedbio.2014.09.031

Semi-automated tracking and continuous diameter monitoring of inferior vena cava in simulated and experimental ultrasound imaging

Luca Mesin, Paolo Pasquero, Stefano Albani, Massimo Porta, Silvestro Roatta

February 9, 2015

Abstract

Assessment of respirophasic diameter fluctuations of the inferior vena cava (IVC) is detrimentally affected by its concomitant displacements. This study aims at presenting and validating a method to compensate for IVC movement artifacts while continuously measuring its diameter in an automated fashion (with minimal interaction with the user) from a longitudinal B-mode ultrasound (US) clip. Performance was tested on both experimental US clips collected from 4 healthy subjects and simulations, implementing rigid IVC displacements and pulsation.

Compared to the traditional M-mode measurements, the new approach systematically reduced errors in caval index (CI) assessment (range over maximum diameter value) by an extent depending on individual vessel geometry, IVC movement and choice of the M-line (the line along which the diameter is computed). In experimental recordings, it identified both the cardiac and respiratory components of IVC movement and pulsatility and evidenced the spatial dependence of IVC pulsatility.

IVC tracking appears a promising approach to reduce movement artifacts and to improve reliability of IVC diameter monitoring.

Keywords: Inferior vena cava, Ultrasound, Tracking

Introduction

Due to its low-cost and non invasiveness, ultrasound (US) imaging of the inferior vena cava (IVC) is increasingly employed as bedside point-of-care methodology in support to the management of fluid therapy in critically ill patients ([25]). Indeed, the respirophasic changes in IVC diameter are related to the volume status. This relationship has been evidenced in different studies investigating the IVC diameter changes: in healthy pediatric subjects [10], in healthy blood donors [16], in critically ill patients [1] and in cases of liver fibrosis or cirrhosis [14]. However, US measurements of the IVC are taken without a standardization of the technique ([21]). Indeed, for example, researchers reported both longitudinal ([2, 5, 8, 7, 9, 13, 16, 17]) and cross-sectional ([3, 6, 17]) imaging approaches. As a result, recommended diagnostic cutoffs vary considerably in the literature ([25]).

Recently, movements of the vessel relative to the US probe during the respiratory cycle were indicated as possibly contributing to this variability ([4]). Indeed, the maximum and minimum diameter values occurring at the end of the expiration and inspiration phases, respectively, are usually computed along a fixed line (referred to as M-line). Since the IVC moves during respiration, these two measurements are taken at different points along the vein, thus introducing an error in the measurement, whose magnitude depends on longitudinal changes in shape and curvature of the IVC. While this movement artifact affects both cross-sectional and longitudinal measurements, only in the latter the actual displacement of the vein can be appreciated. In fact, respiratory displacement of the IVC were shown to be larger than 2 cm along the cranio-caudal direction (average of 70 subjects) and to represent a major source of possible artifact ([4]).

We hypothesized that by tracking the movements of the vein in a longitudinal scan, the IVC diameter could be measured along a line moving with the vein, hence ideally always related to the same vessel cross-section. Accordingly, aim of the study was to develop a semi-automated methodology yielding continuous measurement of IVC diameter, free of the possible artifacts produced by respirophasic displacements of the vein along the longitudinal axis. The study follows three subsequent steps:

- implementation of a vessel tracking algorithm with automated diameter measurement at the site initially chosen by the operator;

- testing of the algorithm effectiveness using simulated data;

- application of the algorithm to experimentally generated data.

Advanced image processing techniques have been specifically developed to track displacements as well as deformations of tissues and organs using US images, e.g., to estimate the movements of the left ventricle ([23]) or to track the motion and deformation of images investigating their speckle ([24]) or to compute the motion out-of-plane and within plane to assist US guided interventions ([15]). In the present paper, a simple algorithm with low computational cost is developed for processing US clips containing a longitudinal scan of the IVC with the following features:

- on the first frame, the operator is asked to select two "salient" reference points to which the IVC is presumably physically "anchored" as well as the M-line whose intersections with the IVC will be used to estimate the diameter;

- the algorithm, by tracking the displacement of the two reference points, follows the movement, the linear deformation and the rotation of the IVC and recalculates the M-line position and orientation accordingly, thus providing, on a frame-by-frame basis, a measurement of the IVC diameter ideally related to the same vessel cross-section;

- the time course of the diameter change is then provided for the whole duration of the clip, with no further intervention by the operator.

This diameter measurement is compared to the "classical" measurement computed along a fixed M-line, both in simulated and experimental data.

Materials and Methods

The method and the simulated and experimental test signals are discussed below.

Inferior Vena Cava tracking and diameter measurement

A software algorithm (Matlab, the Mathworks) was developed to process an US B-mode video clip reporting a longitudinal view of the IVC in order to provide a continuous measurement of the IVC diameter, compensating for possible IVC movements. This is based on a frame-by-frame processing that performs the following tasks:

- tracks IVC movement;

- redraws the section line according to the IVC movement in order to intersect the same IVC portion;

- automatically detects IVC borders and measures IVC diameter.

At the first frame in the clip, the user is asked to select a rectangular portion including a longitudinal view of the IVC (Figure 1). Then, the selected portion of frame is de-blurred by an adaptive Wiener low pass filter, based on statistics estimated from a local neighborhood of each pixel of size 5x5 pixels. On such an image, the user selects two reference points, assumed to be anchoring sites for the vein. They can be independently selected on either the near- or the far-end wall of the vessel. The two reference points are connected by a "reference segment". In Figure 1, the reference point on the left is close to the confluence of the hepatic veins into the IVC, the rightmost one is close to the most caudal level of the first segment of the liver (caudate lobe). Then, the user draws the M-line, i.e. a segment cutting transversally the IVC, which defines site and direction for diameter measurement. The site chosen in Figure 1 is about 2 cm distal to the confluence of the hepatic vein. The diameter was estimated from each frame either on the fixed M-line or along a moving segment, obtained displacing rigidly the M-line together with the reference points (as explained in the following).

The vein is assumed to exhibit smooth movements and deformations in subsequent frames. The position of each reference point is automatically re-mapped in subsequent frames. The estimation of the displacement exhibited by a reference point from one frame to the next is calculated from the comparison of single image portions (size 128x128 pixels) centered on the current position of the reference point in the first frame of the pair. The two portions are aligned in the 2D Fourier domain, in order to avoid the finite resolution limitations that would be encountered if working in the original spatial domain[1]. The alignment is obtained by minimizing (by means of the Newton optimization method) the mean squared difference between the transformed and phase shifted images, after cropping

---

[1]A displacement in the space domain is associated to a phase shift in the Fourier domain. Such a phase shift could be any number, it is not limited to be a sampling point. Thus, an image can be shifted with infinite resolution in the Fourier domain by the following method: transform the image, apply the phase shift and come back to the spatial domain by inverting the transformation.
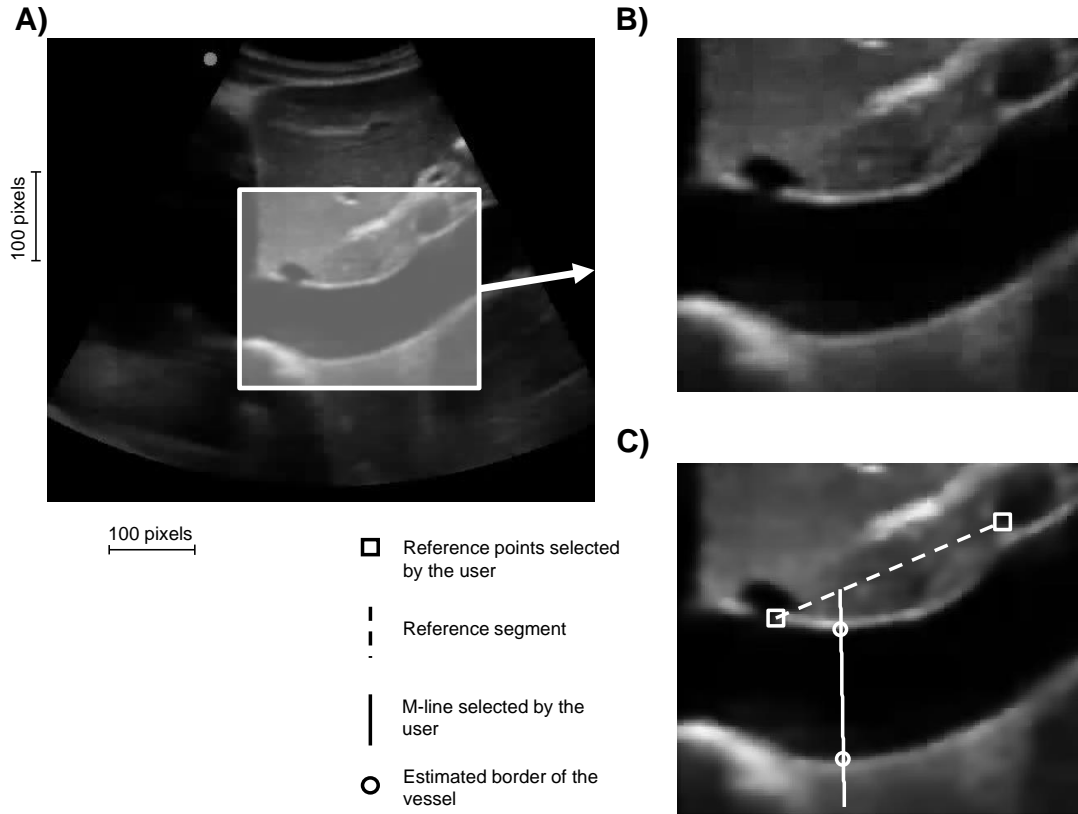
Figure 1: Example of user settings on the first frame of the clip showing a longitudinal view of the IVC. A) identification of the rectangular portion containing the IVC. B) Enlargement of the selected portion which is used for further processing. C) On the smoothed image (see text), the user selects the two reference points (open squares) and draws the M-line (continuous line). Based on these settings, the program defines the reference segment (dashed line) used to track the IVC displacement in subsequent frames and identifies the vessel borders along the M-line (open circles) used for estimating the IVC diameter.

them (20 pixels each side), in order to avoid edge effects (thus, the maximal displacement of the vein between two subsequent frames has to be less than 20 pixels).

Given the new position of the reference points, the new reference segment is calculated. It may appear translated, rotated as well as stretched in the horizontal and vertical directions, as compared to its position in the previous frame. On this basis, the M-line is recalculated by maintaining its geometrical relation with the reference segment, i.e., by keeping constant their angle of intersection as well as the ratio of the distances between the intersection point and the two reference points. In this way the M-line should follow movements and deformations of the IVC and ideally intersect the IVC always along the same cross-section.

Once the M-line is re-positioned, the US intensity along the line is computed by interpolation, obtaining a 1D function. Such a function is first transformed by an affine map in order to limit its dynamic range between 0 and 1; then it is processed by an arctangent function, to emphasize the rapid variations. Then, the borders of the vessel are detected as the points in which such rapid variations are identified as points of local maximal absolute derivative. In order to exclude possible spurious points, the values located closest to the vessel border in the previous frame are selected.

Dataset

The method was tested on both simulated and experimental data.

1. Simulations

Different simulations were implemented in order to test the performance of the algorithm. Video clips were constructed based on a single frame extracted from a real US scan of the IVC along the longitudinal axis (see the following Section on the Experimental data). Subsequent frames were obtained by progressive alterations of the initial image in terms of displacement/rotation and vertical scaling, in order to simulate the movements of the vein (in the sagittal plane) and its diameter variations, respectively. To this aim, the original frame was cropped around the portion of vein to be considered and was subjected to single or multiple alterations, i.e. translation, slight rotation, vertical scaling and corruption by additive noise (see below). Then single pixel values in the new frame were obtained from the altered original frame by interpolation.

Based on the literature ([4]) and on personal observations, we related the horizontal IVC displacements and the diameter variations to the (periodic, low frequency, $f_{resp} = 0.3$ Hz) respiratory activity and to the (periodic, high frequency, $f_{heart} = 1$ Hz) heart pulse. Thus the IVC position was periodically changed with different frequency values for the different movement components. Moreover, a small additional periodic rotation and a vertical displacement were introduced with a different frequency, in order to obtain always different simulated frames in subsequent respiratory cycles (they could represent a motion of the patient or of the operator). Video clips were thus generated with a frame rate of 10 Hz and a duration of 30 s, resulting in 300 frames for each simulation; a relatively low frame rate is chosen for increasing IVC displacement in subsequent frames thus further

challenging the performance of the tracking algorithm. Four simulations were performed with increasing complexity.

- Simulation 1. Displacement along the horizontal (x) and the vertical (y) directions (corresponding to the cranio-caudal and the antero-posterior directions, respectively), defined respectively as

$$D_x = 30 \sin(2\pi f_{resp} t) \qquad D_y = 5 \sin(2\pi t/10) \tag{1}$$

  where t is the time variable and the displacements are measured in pixels.

- Simulation 2. A slight rotation was implemented in addition to the displacement described above (which represents a change in the inclination of the IVC longitudinal axis in the sagittal plane), with an angle

$$\theta = 0.1 \sin(0.3\pi t) \tag{2}$$

- Simulation 3. A vertical scaling was implemented in addition to the translation and rotation described in the previous points, according to the following scaling factor

$$S = 1 + 0.1 \sin(2\pi f_{heart} t) + 0.1 \sin(2\pi f_{resp} t) \tag{3}$$

- Simulation 4. The same as Simulation 3, but corrupted by an additive Gaussian noise, with zero mean and variance equal to 0.1%, 1% or 3% of the frame intensity range, in three different simulations.

The simulated ranges of motions were selected in order to get a dynamics similar to the experimental one. The simulated video clips assembled in this way were processed as described above by the tracking algorithm, yielding a measure of the IVC diameter along a moving M-line, anchored to the moving IVC. This measurement was compared to the one obtained along a fixed M-line, i.e. the one originally drawn by the user on the first frame, maintained in the same position and direction (relative to the US probe), as occurs in standard M-mode assessments. Diameter measurements were normalized with respect to the initial value for easier comparison and low pass filtered (anti-causal Butterworth filter of order 4 with cutoff frequency at 2 Hz) in order to remove the quantization noise generated by the discrete pixels. Then, the following performance indexes were used.

- Root mean square (RMS) error of the difference between the estimated and simulated variation of the diameter, given as percentage of the first value. Moreover, for Simulations 3 and 4, the error was also compared to the simulated diameter variation (which is not included in Simulations 1 and 2), indicating the percentage error with respect to the standard deviation of the simulated scale.

- Caval index, defined as

$$CI = \frac{max(D) - min(D)}{max(D)} \tag{4}$$

  where D indicates either the estimated or simulated IVC diameter.

2. Experimental data

Two dimensional (B-mode) longitudinal views of the IVC were recorded from 4 healthy volunteers (one female, three males; age, mean±std 29±11 years; height 180±13 cm; weight 66±10 kg; BMI 20.4±0.3 kg/m^2). All subjects provided written informed consent for the collection of data and the subsequent analysis, according to the Declaration of Helsinki. The US investigation was carried out with a system (M-Turbo Ultrasound System, SonoSite, Inc., Bothell, WA, USA[2]; frame rate 30 Hz, resolution 0.4 mm per pixel, 256 grey levels) equipped with a 2-5 MHz curvilinear probe. B-mode longitudinal views of the IVC were taken with a subxifoideal approach, with the subject in the supine position during relaxed normal breathing. Video clips lasting 10 s were recorded for off-line processing (as described above). The site chosen for the measurement was approximately 2 cm distal to the confluence of the hepatic vein ([21, 11]).

Results

Figures 2-5 show the application of the method to the simulations (described in Section Materials and Methods - Dataset - 1. Simulations). Examples of frames are shown, indicating the reference points and the estimated diameter along fixed or moving M-lines. At the bottom of the figures, the estimated diameter for each frame (normalized with respect to the first value) is shown, together with the simulated scaling along the y direction (see the Section Materials and Methods - Dataset - 1. Simulations for details).

In Figure 2, only translations of the vein are simulated (Simulation 1 described in Section Materials and Methods - Dataset - 1. Simulations). The method performs a perfect alignment of the reference points, so that the movements of the vein are strictly followed and the diameter estimated on the moving reference system (along the moving M-line) is unaffected by the IVC movement: the RMS error with respect to the simulated (unchanged) diameter is at the level of the round-off numerical error. On the other hand, the diameter estimated along the fixed M-line is affected by the movements of the vein because, in the different frames, it involves different sections of the IVC (see the dotted M-line in the frames of Fig. 2A). In this case, the maximum error is larger than 10% and the average RMS error is 4.4%. Since in this simulation only rigid translation of the IVC are simulated the theoretical caval index (CI) is 0%. However, due to the above mentioned movement-related error in diameter estimation by the fixed M-line a CI of 14.6% is obtained. Thank to the effective tracking of the IVC movement a CI of 0.0% is instead detected along the moving M-line.

Figure 3 shows the results of Simulation 2, which implements both translations and rotations of the vein. As shown in Fig. 3B, this pattern of movement introduces a small artifact in the moving M-line estimation (dashed line), RMS error being 0.8%. However, it remains considerably smaller than that related to the fixed M-line: RMS= 5.3%. Also in this case, no IVC pulsation is simulated (i.e. theoretical CI equal to 0%), however an

---

[2]M-Turbo Ultrasound System - User manual, http://www.sonosite.com/downloads/M-Turbo_UG_P07662.pdf

A)

Frame number 1

Frame number 60

100 pixels

□ Reference points

○ Estimated border of the vessel (fixed M-line)

⋮ Estimated interior of the vessel (fixed M-line)

Frame number 105

Frame number 160

◁ Estimated border of the vessel (moving M-line)

▮ Estimated interior of the vessel (moving M-line)

100 pixels

B)

Variation of diameter estimated from each frame

estimated (moving M-line)

simulated

Normalized units

1.0

0.9

estimated (fixed M-line)

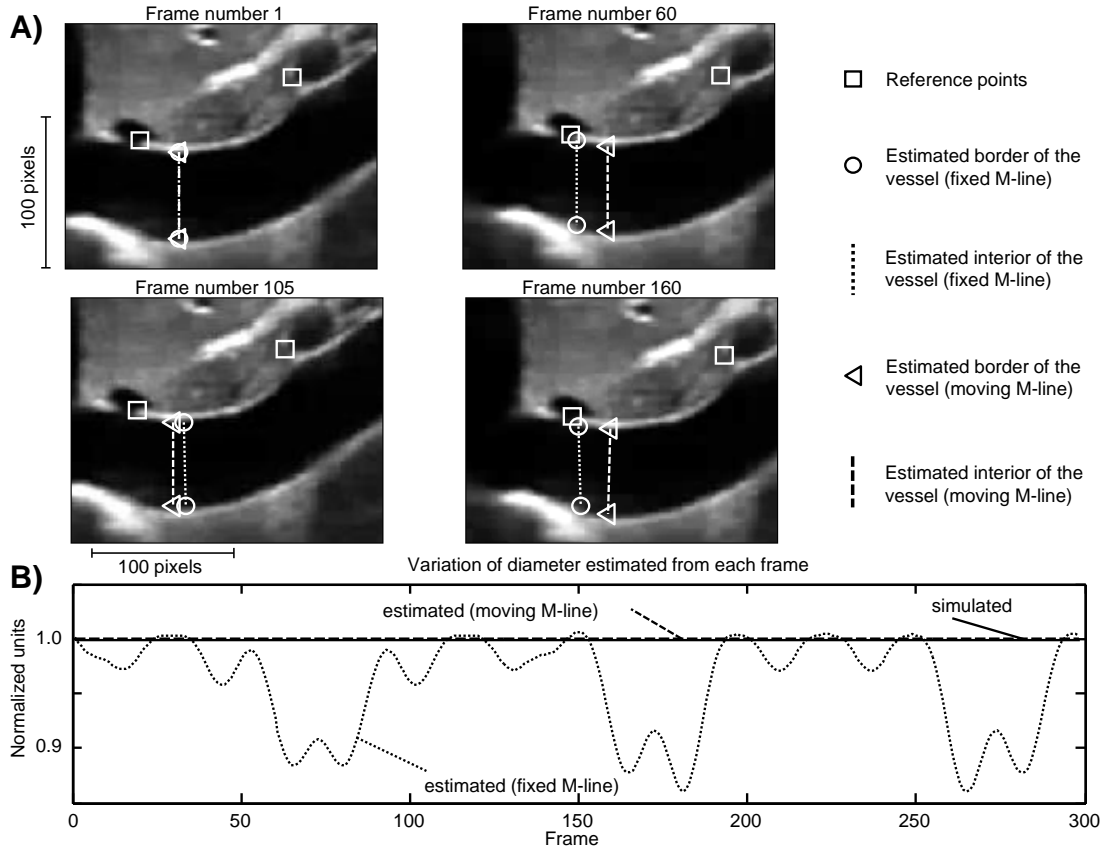0   50   100   150   200   250   300

Frame

Figure 2: Processing of simulated data according to Simulation 1 (Section Materials and Methods - Dataset - 1. Simulations), consisting in simple vertical and horizontal translations of the initial image. A) Four frames extracted from the simulated clip are presented, with the indication of the reference points and of the borders of the vein detected along the fixed or moving M-line (the latter being anchored to the reference points which track the simulated movements of the IVC). B) Simulated and estimated variation of the vein diameter across different frames. The simulation implements only linear displacements of the image, leaving the vessel dimensions unaffected (continuous line). Note that the diameter estimated along the fixed M-line (dotted line) is heavily affected by the IVC displacement while the measurement along the moving M-line (dashed line) is extremely constant, faithfully reproducing the simulated (constant) diameter.

estimated CI of 17% results from the fixed M-line. The error is markedly reduced in the estimation performed along the moving M-line (CI equal to 3.6%).

The results of Simulation 3, implementing translations, rotations and vertical scaling of the vein are displayed in Figure 4. At difference from previous simulations, a change in diameter is now simulated by the periodical vertical scaling of the image and is depicted by the continuous line in Fig. 4B. The diameter was estimated along the fixed or the moving M-line. The RMS errors are 5.3% for the fixed line and 1.0% for the moving one (by normalizing these values with respect to the standard deviation of the implemented scaling, the RMS errors become 52.8% for the fixed M-line and 10.2% for the moving one). The estimated CI was 36.7 and 32.1% for the fixed and moving M-line, respectively; the simulated value was 33.2%.

Figure 5 shows the application of the method to noisy frames, obtained by perturbing with additive Gaussian noise the data of Simulation 3 including translations, rotations and scaling of the initial image (Simulation 4 described in Section Materials and Methods - Dataset - 1. Simulations). By increasing the amount of noise (i.e., the variance of the additive Gaussian noise), the estimates become progressively affected by a larger error. In particular, the estimation of the reference points is degraded by the noise (notice the large error in estimating the rightmost reference point on the frames number 80 and 160, for the most noisy condition). However, errors of the measurements performed along the moving M-line are always lower than along the fixed M-line (as shown in Figure 5B and 5C). The estimated CIs, at increasing noise level, were 39.4, 37.7 and 40.1% for the fixed M-line and 32.1, 33, 32% for the moving M-line; the simulated value was 33.2%.

The tracking algorithm was then applied on longitudinal B-mode scans of the IVC collected from 4 healthy subjects. As shown in Figure 6 for the different subjects, the extent of IVC displacement is in the order of 20 and 10 pixels (i.e. 8 and 4 mm) in the longitudinal and vertical direction, respectively. In all subjects the movement exhibited in the sagittal plane appears to roughly follow a diagonal path during respiratory phases. On top of this large movement, a smaller oscillatory component at about 1 Hz, corresponding to the heart rate, is also visible, particularly on the time course of the angle of rotation. In subject 4, the contribution of the heart is larger than in the others and clearly affects both the estimated displacement and the rotation angle.

Figure 7 shows the different diameter measurements obtained by adopting a fixed or a moving M-line. Although the average difference between the two approaches is not so large (between 0.63 and 2.27 pixels, corresponding to 0.25 and 0.90 mm, respectively), the maximum difference can be as large as 8.5 pixels (corresponding to 3.4 mm). Because of this latter effect, the differences between the estimates of the CI in the two conditions vary between 0.5% (subject 1) and 8.2% (subject 4). Estimated CIs were the followings: 18 and 18.5% (subject 1), 39.9 and 36.1% (subject 2), 43.7 and 40.2% (subject 3), 32.6 and 24.4% (subject 4), as obtained for the fixed and the moving M-line, respectively.

In order to show to what extent the choice of the fixed M-line may affect the CI assessment, also depending on the individual IVC anatomical profile, both simulation and experimental recording were reprocessed for subject 2 (exhibiting a saber IVC profile) and the results are shown in Figure 8. In Fig. 8A, the Simulation 3 was operated based on frame number 1 of subject 2 (instead of subject 1, as done before): the simulated
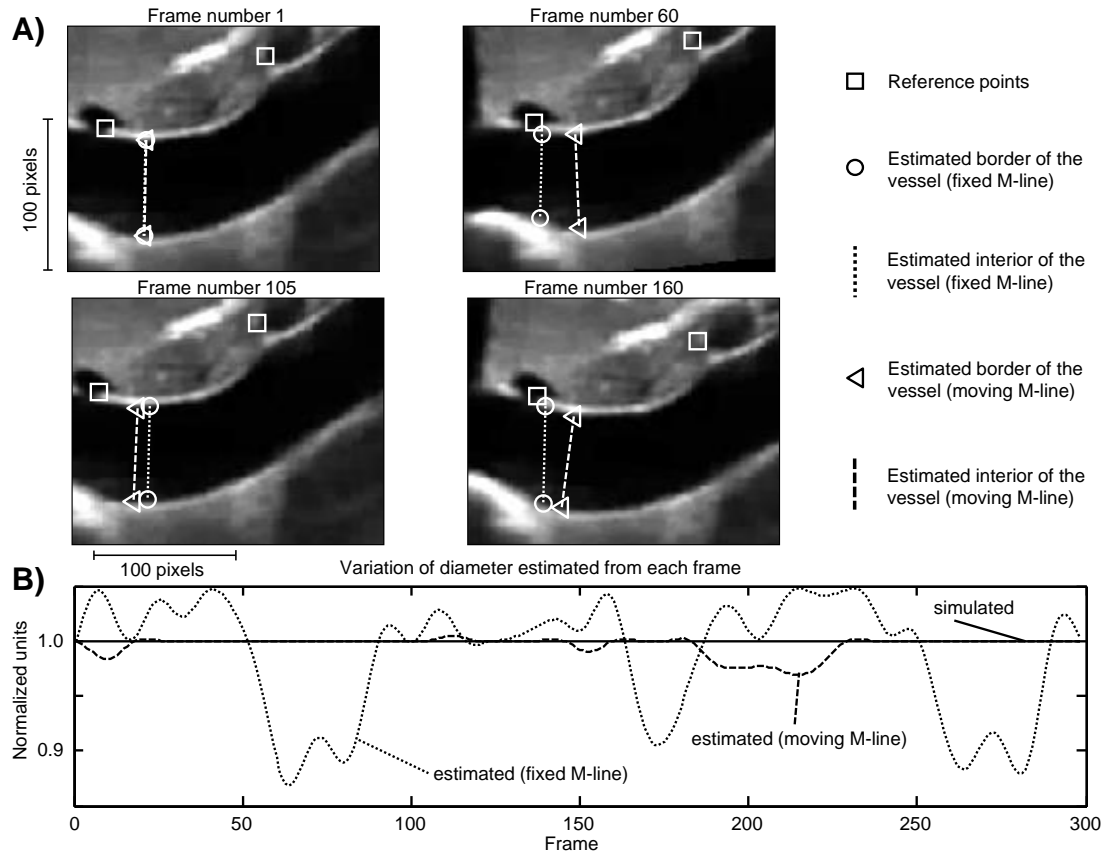
Figure 3: Processing of simulated data according to Simulation 2 (Section Materials and Methods - Dataset - 1. Simulations), consisting in both translation and rotation of the initial image. A) Four frames extracted from the simulated clip show the relocation of reference markers and moving M-line, tracking the simulated IVC movement. B) Simulated and estimated variation of the vein diameter across different frames as described in Fig. 2. Also in this case, there is no simulated variation of the diameter (IVC distortion) and the change in the diameter detected along the fixed or the moving M-line results from (simulated) movement artifacts.
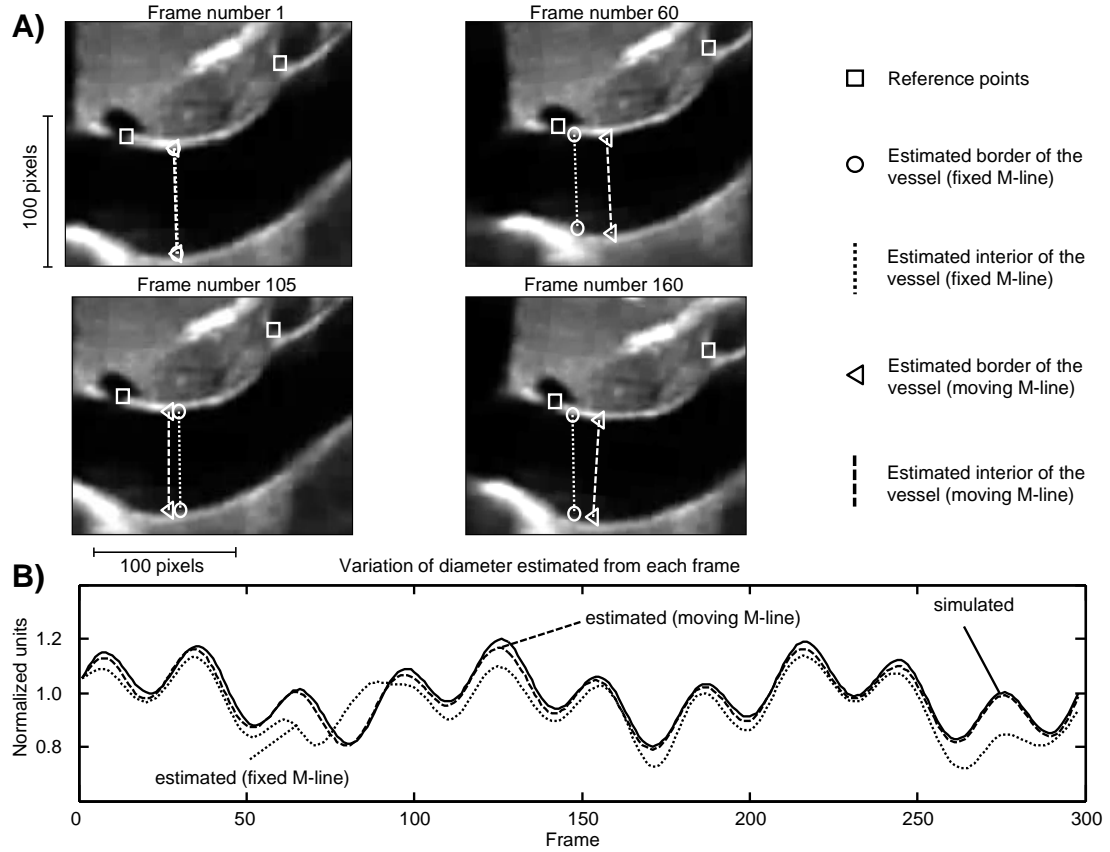
Figure 4: Processing of simulated data, obtained by translating, rotating and scaling along the vertical axis the first frame of a measurement (as described in Section Materials and Methods - Dataset - 1. Simulations, Simulation 3). A) Four frames extracted from the simulated clip, as described in Fig. 2. B) Simulated and estimated variation of the vein diameter across different frames, as described in Fig. 2. Note that in this case the simulated changes in diameter are also implemented, as shown by the continuous line.
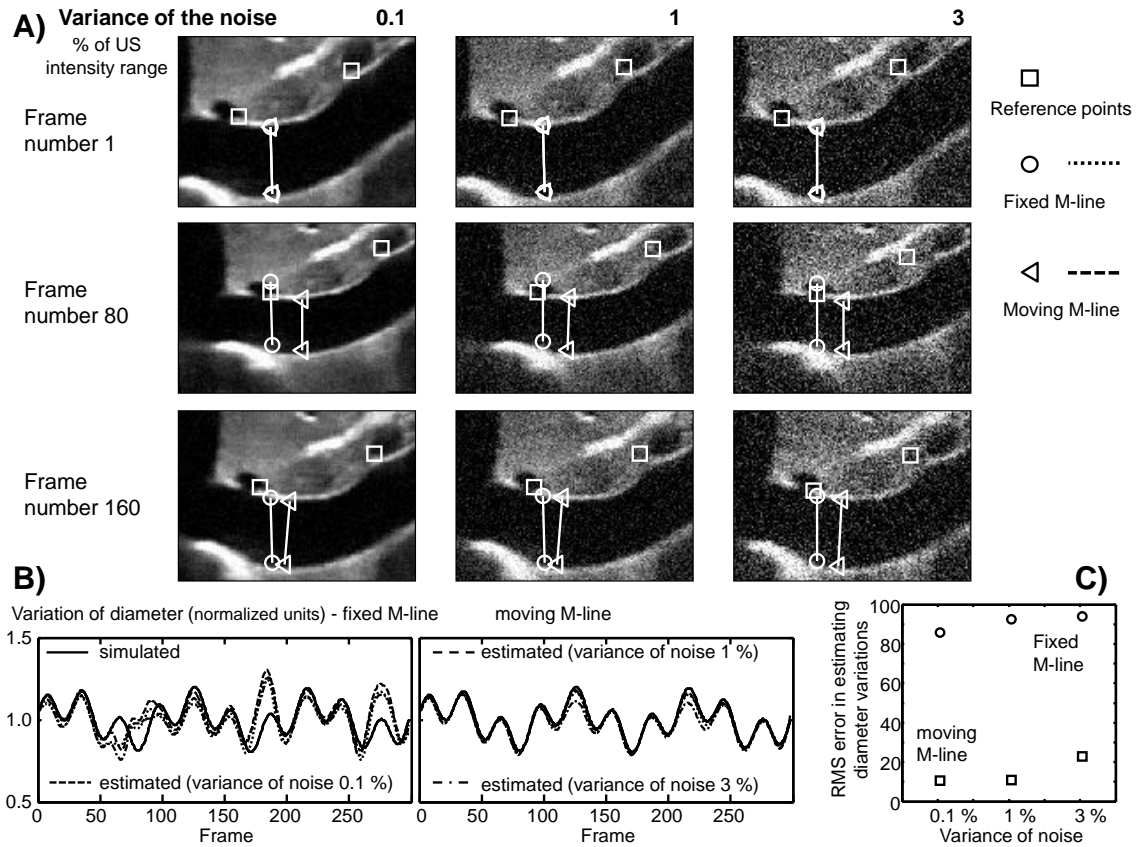
Figure 5: Processing of simulated data, obtained by adding Gaussian noise at different levels to the data considered in Figure 4 (as described in Section Materials and Methods - Dataset - 1. Simulations, Simulation 4). A) Example of 3 frames extracted from simulated clips with different levels of additive noise; indications as in Fig. 2. B) Simulated and estimated variation of the vein diameter across different frames and C) RMS errors of the estimations (normalized with respect to the standard deviation of the simulated scale), for the fixed line and the moving one, as a function of the variance of the additive noise.
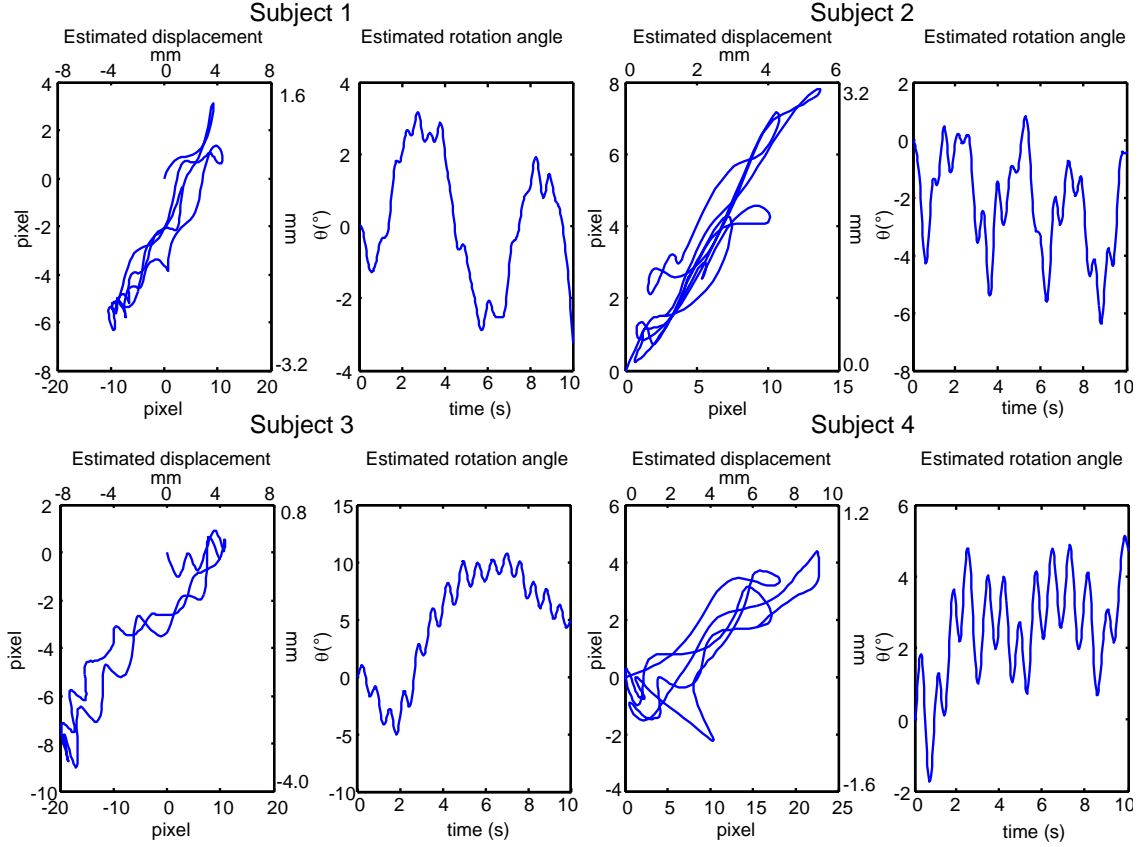
Figure 6: Displacement and rotation of the vein estimated from longitudinal US scans of the IVC on four healthy subjects (Section Materials and Methods - Dataset - 2. experimental data). The displacement of the vein is represented as the trajectory of the mean point between the estimated positions of the reference points, fixed to (0, 0) in the first frame. The rotation represents the change in inclination of the reference segments with respect to the first frame.
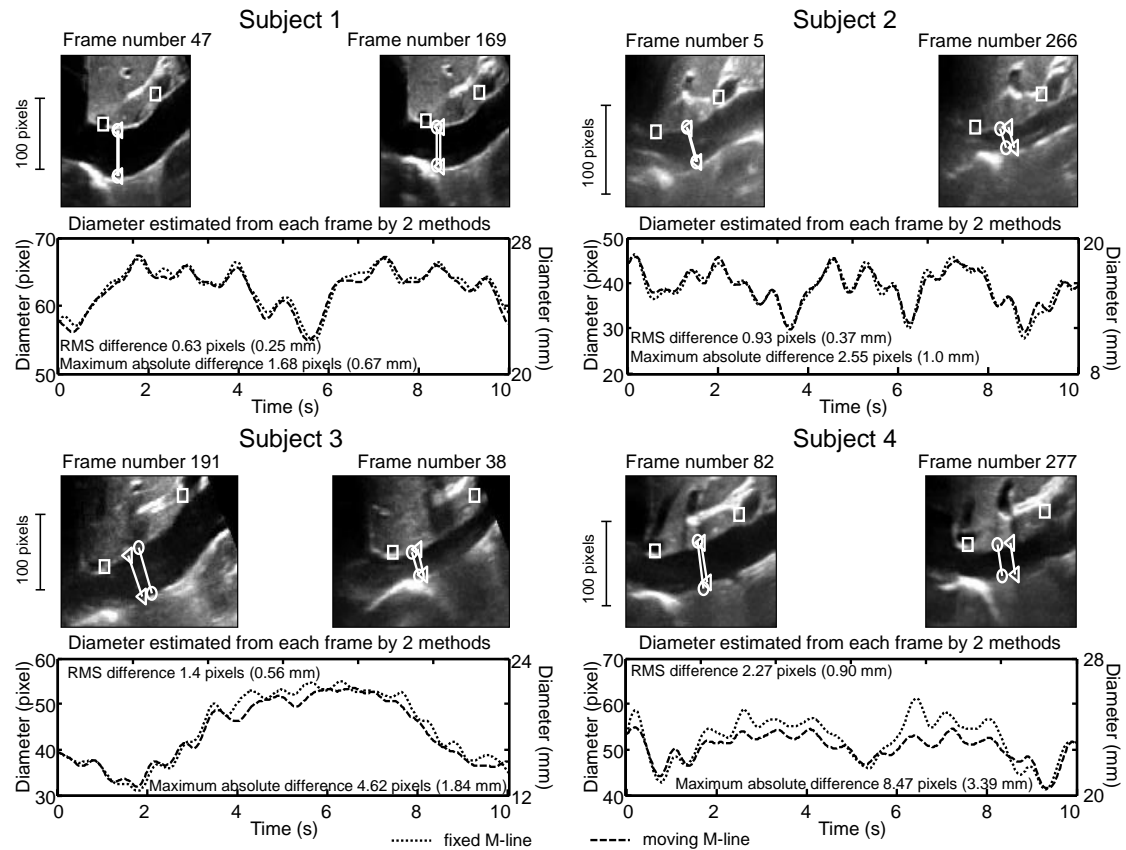
Figure 7: Diameter estimation in four healthy subjects. The fixed and moving M-lines were initially positioned on the same optimal location, quite far from the reference points, orthogonal to the vein in the first frame and in a region in which the contrast of the vein border was quite high. For each subject, two representative frames are presented and the diameters estimated along the fixed and moving M-line are shown (together with an indication of the average and maximal difference). The two frames presented correspond to the moment in which the diameter estimation is either maximally positive or negative.

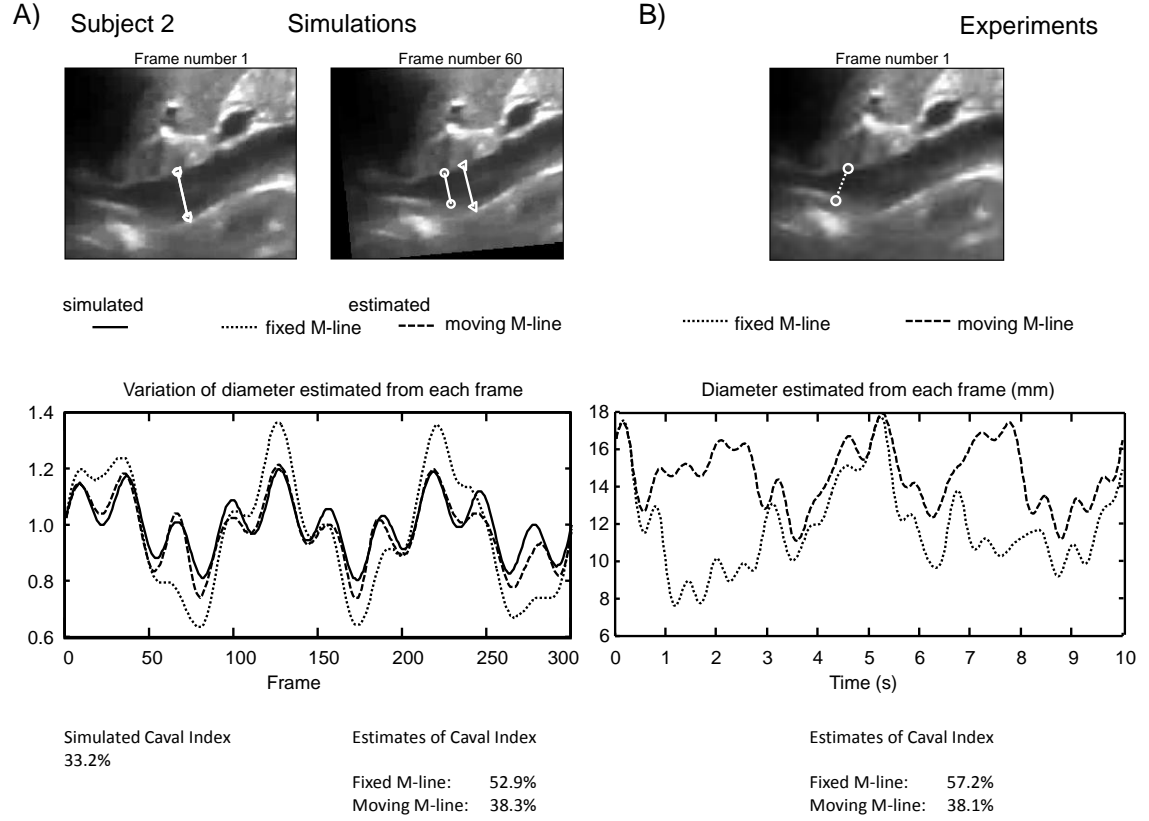Figure 8: Processing of simulated and experimental data from subject 2, presenting a IVC with a saber shape. A) The simulations were obtained by translating, rotating and scaling along the vertical axis the first frame of a measurement (as in Figure 4, where subject 1 was considered). B) Experimental data processed considering a specific M-line, chosen in the region in which the vein is narrowing.

translatory and rotatory movements greatly affect the IVC assessment along the fixed M-line, as it gets closer to IVC narrowing, while the measurement performed along the moving M-line still closely reproduces the simulated IVC changes (Fig. 8A). Similarly, in experimental recordings (again from subject 2) placing the fixed M-line close to the narrowing point introduces a disparity between moving and fixed M-lines resulting in a large difference between the CIs estimated by the two approaches (Fig. 8B; this is in contrast with results shown in Figure 7, in which the M-line was chosen in a portion of the vein in which the diameter was uniform).

Finally, in the same 4 subjects, the IVC diameter was simultaneously estimated in 3 different sections by means of 3 corresponding moving M-lines controlled by the same algorithm. The results are presented in Figure 9. Notice that the time course of IVC diameter varies in the different sections in the same subject, demonstrating that different portions of the IVC exhibit different pulsatility. As a consequence, the CI estimated in
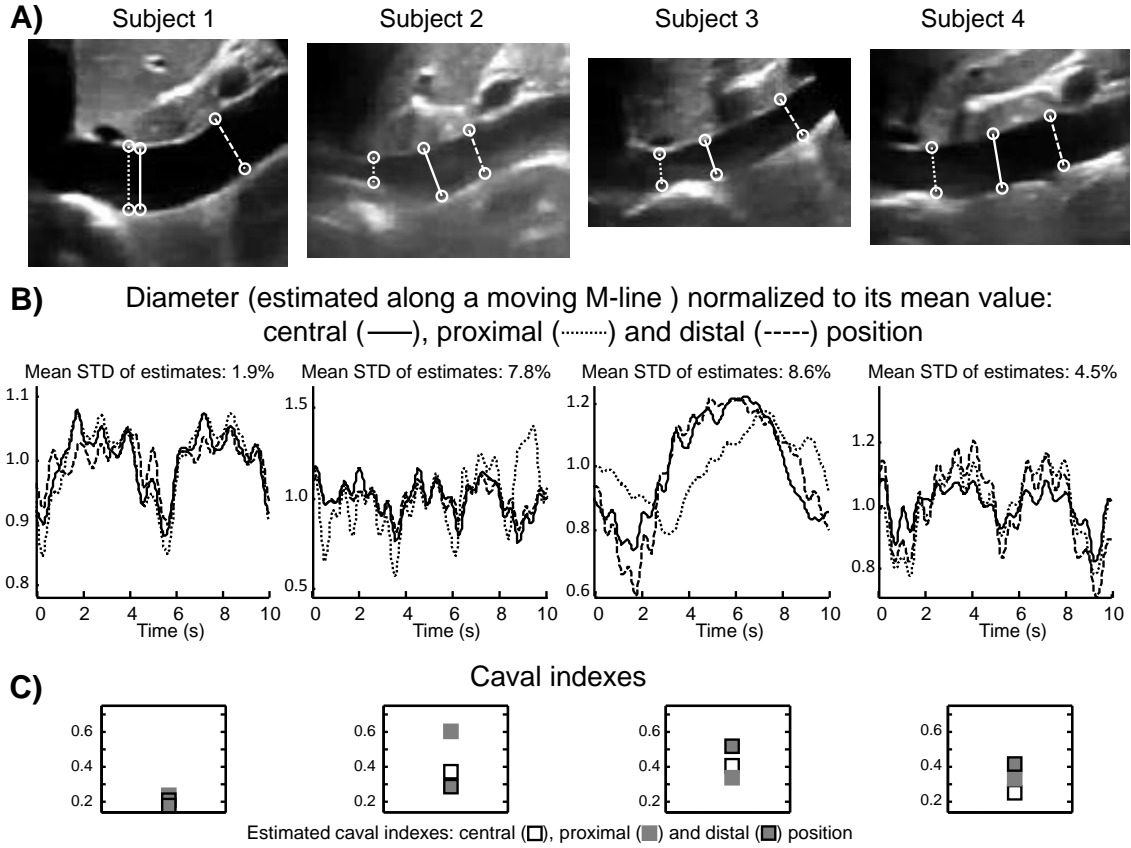
Figure 9: IVC diameter estimation performed along 3 different moving M-lines in 4 subjects. A) First frame of the clip indicating the initial position chosen for the 3 M-lines: proximal (dotted), central (continuous, the same of Fig. 7) and distal (dashed). B) Time course of the diameter changes detected by the three M-lines; note the different patterns exhibited. C) The CI estimated from the traces presented in B, corresponding to the different selected sections of the IVC.

the three positions presents a large variability, although with some difference among the 4 subjects.

Discussion

The assessment of IVC dimensions based on US scans is potentially affected by the movements of the vein, which mainly occur in the cranio-caudal direction, due to respiratory activity ([4]). In order to avoid respiration-related movements, in a recent study the recordings were performed on subjects maintaining a short apnea, thus limiting the analysis of oscillations to the cardiac component ([18]). Another possibility is to manually make single measurements at the same location using B-mode cine-loop rather than M-mode ([21, 16]). However this approach, based on discrete measurements, cannot provide

a continuous monitoring of the IVC diameter.

In this study, an image processing algorithm is presented, which operates on longitudinal scans of the IVC (B-mode clip) and, based on reference points arbitrarily selected by the user, is able to follow the IVC displacement in time. In this way, diameter changes of a given IVC section can be monitored irrespective of IVC longitudinal movements and the analysis can be oriented to both cardiac and respiratory-related oscillations. The algorithm was validated in a series of simulations in which translation, rotation, distortion of the IVC and additive noise were progressively implemented. The results showed that

- simulated displacement of the IVC generated in fact movement artifacts in the diameter estimation performed along a fixed M-line (as provided by most commercial devices operating in M-mode),

- the algorithm is able to eliminate most of the movement artifacts by performing the measurement along the moving M-line, which follows the IVC displacements,

- relatively small errors expressed in terms of average RMS of measured-simulated diameter may however result in large changes in the estimated CI,

- the movement related errors depend not only on the extent of the movement, but also on the individual longitudinal IVC profile, as well as on the chosen M-line (compare subject 2 in Figure 7 and 8).

Technical considerations

A simple, fast method was used (about 2 frames were processed in 1 s, using a Matlab implementation of the algorithm, on an Intel(R) Core i7, with clock frequency of 2 GHz, 6 GB of RAM and 64 bits operating system). It estimates the translation of the two reference points in the Fourier domain in order to overcome resolution problems. One possible extension of the method would be to track the motion of more than 2 reference points. This is likely to improve the description of IVC deformation and the stability of the estimates but with increased comutational costs[3]. A further possible improvement, also increasing the computational cost, could be achieved by estimating also the rotation of the patch of frame around the reference points, together with its translation. Finally, the deformation of either the whole frame or the considered portions around the reference points could be investigated ([24]). However, in order to keep the method fast and simple, only translations were estimated, as they were the most important variations in the considered subsequent patches, due to the high frame rate and the small dimension of the patches.

---

[3]An attempt was made to use 4 reference points on Simulation 4 at the highest noise level (shown in Fig. 5). The 4 points were independently tracked and grouped into 2 couples. Two new reference points were obtained from the barycenter of each couple and the rest of the processing was unaltered (as described in the Methods section). RMS was reduced from 23.8% to 15.8% and computational cost increased by 80%, as compared to using only 2 reference points (unpublished observation).

Interpretation of the results

The results of Simulation 1 and 2 clearly indicate that when the IVC diameter measurement is performed by means of the classical M-mode (i.e. along a fixed M-line), set on a longitudinal view of the IVC, movement artifacts are introduced. In fact, diameter variations were detected in the absence of any simulated change of the vessel's dimension. These artifacts were quantified by an average RMS error of 4-5%. A larger mistake (in the range 5-10%) was obtained when a variation of the diameter was also included (Simulation 3) and in the case of noisy simulations (Simulation 4). The error in estimating the dynamics of the diameter reduces the accuracy of the estimates of indexes which could be extracted from it. As an important example, the CI was considered here. When considering noisy simulations including movements and scaling of the vein (Figure 5), the estimates of the CI were about 38-40% for the standard method and around 33% with the new one (about 20% variation). In experiments (Figure 7), the maximum variation of the CI computed by the two methods was found for subject 4: 24% instead of 32% (25% of variation). These differences were observed considering only 4 healthy subjects and thus cannot be representative neither of the healthy nor of the pathological population. On the contrary, individual characteristics may well produce larger movement artifacts, according to the following considerations.

1. As already pointed out in the Results section, the ensuing error in the estimation of the CI can be considerably larger than the RMS error. This is due to the definition of the CI, which is based on single measurements in the diameter curve, the maximum and minimum, occurring at the end of expiration and inspiration, respectively ([4]), exactly when the maximal displacement of the IVC also occurs.

2. The image (from subject 1) adopted for the simulations was characterized by a rather uniform diameter of the IVC. However the single simulation based on subject 2 (Fig. 8A) shows that large variations are obtained if the diameter of the vein is not uniform. Indeed, the movement artifact in the diameter estimation also depends on the anatomical morphology of the IVC and dramatically increases if the fixed M-line is located in proximity of a narrowing or of a curvature of the vessel (compare subject 2 in Fig. 7 and Fig. 8B). In addition, other individual characteristics such as depth and type of respiration (thoracic vs. diaphragmatic) determine the extent of IVC movement, thus potentially affecting the measurement ([12]). Indeed, the reliability of the assessment of fluid responsiveness using US was found to be higher in controlled mechanical ventilation than in spontaneously breathing patients [25]. Notice also that the veins of the healthy subjects included in this study made small movements (about 1 cm of cranio-caudal displacement, whereas the average displacement of the patients investigated in ([4]) was larger than 2 cm and the maximum displacement was over 5.5 cm). All these factors, which likely contribute to the large inter-individual variability of these assessments, are counteracted by the adoption of a tracking algorithm that follows the movements of the IVC and anchors the (moving) M-line to the moving IVC (e.g., see the CI estimated by moving versus fixed M-line in Fig 8).

Implications and hints for future studies

By analyzing each single frame, it is possible to appreciate the full time course of the IVC diameter and to detect and discriminate the two main oscillatory components (Figures 6-8): the respiratory and the cardiac rhythms ([18]). The asynchronous summation of the two components introduces a variability in the maximum and minimum diameter measured at each respiratory cycle, which in turn produces uncertain estimates of the CI. By separating the two components, their specific amplitude of oscillation could be computed, possibly achieving increased repeatability of the estimates. In addition, this could provide increased information of possible clinical relevance: the cardiac oscillation is expected to essentially reflect the compliance of the IVC, which in turn reflects the extent of filling of the vascular system; on the other hand, the respiratory oscillation depends on both the IVC compliance and the amplitude and type of respiration (thoracic or diaphragmatic, [12]). A recent study investigating the cardiac component during short apnea seems to support this hypothesis ([18]). New studies, possibly based on the present approach, may elucidate the different functional significance of cardiac and respiratory rhythms in the IVC diameter.

A further critical issue in the assessment of diameter oscillations of the IVC is that they are not equally exhibited by the different tracts of the vein. As often observed in longitudinal scans, some parts of the vein, possibly anchored to other structures (e.g., diaphragm or vein inlets), appear more rigid than others, thus exhibiting smaller changes in diameter. For instance, [21] reported a lower CI at the level of the diaphragm (20%) compared to more caudal sites, such as hepatic vein inlet (30%) and left renal vein inlet (35%). These observations are confirmed by the results of Figure 9, showing that the assessment of the diameter variations along three distinct (moving) M-lines results in considerably different CIs. In the literature, there are non univocal recommendations about where to perform the diameter measurement ([21, 20]): this inhomogeneous behavior of the vessel is likely to contribute to the variability of the assessments ([22]).

This approach, allowing for simultaneous monitoring of IVC diameter over several IVC sections could be employed to compute the average oscillation exhibited by a whole IVC segment, or alternatively, to compute changes in the area of the longitudinal IVC section. If the CI were computed on the area, it would likely provide more stable and reliable assessments of the vein's behavior. This possibility has never been tested and could be investigated in future studies.

Limitations

A first limitation concerns the tracking method implemented to follow the reference points: the new position (i.e., related to the new frame) of the reference point is obtained by looking for the best match between a simple translation of the old reference point and the new frame, i.e. no rotation is implemented. Introducing also the possibility of following rotations of each reference point would have probably increased the accuracy in the tracking performance. However, the simplified algorithm here implemented adequately tracked IVC movements in the 4 tested subjects. Moreover, although the algorithm was tested on

healthy subjects, it is expected to work equally well in patients, provided reference points can be identified and the SNR of the clip is acceptable.

Another limitation concerns more in general the longitudinal approach to IVC diameter monitoring, i.e. the impossibility to follow latero-lateral movements of the IVC or to rule out small changes in the inclination of the probe. In fact, latero-lateral IVC displacements of the vein would produce variations of the height (width) of the vessel in the B-mode longitudinal scan, which are impossible to discriminate from real variations of the antero-posterior IVC dimension ([4]). This limitation is intrinsic to the longitudinal approach and is only solved by adopting a cross-sectional approach, which however has other limitations, namely, it fails to detect respiratory displacements of IVC ([4]).

Conclusions

The diameter of the IVC can be investigated noninvasively with ultrasound (US) techniques and provides valuable clinical information on the intravascular volume status of patients. However, this methodology is not standardized and affected by important artifacts, such as those induced by longitudinal movements of the IVC during respiration. A simple methodology has been presented and validated that effectively tracks the IVC displacements in the antero-posterior direction. This virtually eliminates a major source of variability in the M-mode assessment of IVC pulsatility, based on longitudinal scans. In addition, by providing a continuous and semi-automated monitoring of IVC diameter, the algorithm allows for the identification of both cardiac and respiratory oscillatory components of IVC diameter. It is expected that these methodological improvements will reduce the variability and the operator-dependency in the clinical assessment of IVC pulsatility and will thus increase reliability of US imaging in support to the management of fluid therapy in critically ill patients.

References

[1] Akkaya, A., Yesilaras, M., Aksay, E., Sever, M., Atilla, O.D., The interrater reliability of ultrasound imaging of the inferior vena cava performed by emergency residents, Am J Emerg Med., 2013, 31, 10, 1509-1511

[2] Barbier, C., Loubieres, Y., Schmit, C., Hayon, J., Ricome, J.L., Jardin, F., Vieillard-Baron, A., Respiratory changes in inferior vena cava diameter are helpful in predicting fluid responsiveness in ventilated septic patients, Intensive Care Med, 2004, 30, 9, 1740-1746

[3] Blehar, D.J., Dickman, E., Gaspari, R.B., Identification of congestive heart failure via respiratory variation of inferior vena cava diameter, Am J Emerg Med, 2009, 27, 1, 71-75

[4] Blehar, D.J., Resop, D., Chin, B., Dayno, M., Gaspari, R.B., Inferior vena cava displacement during respirophasic ultrasound imaging, Critical Ultrasound Journal, 2012, 4, 18, 1-5

[5] Brennan, J.M., Ronan, A., Goonewardena, S., Blair, J.E., Hammes, M., Shah, D., Vasaiwala, S., Kirkpatrick, J.N., Spencer, K.T., Handcarried ultrasound measurement of the inferior vena cava for assessment of intravascular volume status in the outpatient hemodialysis clinic, Clin J Am Soc Nephrol, 2006, 1, 14, 749-753

[6] Chen, L., Hsiao, A., Langhan, M., Riera, A., Santucci, K.A., Use of bedside ultrasound to assess degree of dehydration in children with gastroenteritis, Acad Emerg Med, 2010, 17, 10, 1042-1047

[7] Feissel, M., Michard, F., Faller, J.P., Teboul, J.L., The respiratory variation in inferior vena cava diameter as a guide to fluid therapy, Intensive Care Med, 2004, 30, 9, 1834-1837

[8] Fields, J.M., Lee, P.A., Jenq, K.Y., Mark, D.G., Panebianco, N.L., Dean, A.J., The inter rater reliability of inferior vena cava ultrasound by bedside clinician sonographers in emergency department patients, Acad Emerg Med, 2011, 18, 1, 98-101

[9] Grant, E., Rendano, F., Sevinc, E., Gammelgaard, J., Holm, H.H., Gronvall, S., Normal inferior vena cava: caliber changes observed by dynamic ultrasound, AJR Am J Roentgenol, 1980, 135, 2, 335-338

[10] Haines, E.J., Chiricolo, G.C., Aralica, K., Briggs, W.M., Van Amerongen, R., Laudenbach, A., O'Rourke, K., Melniker, L., Derivation of a pediatric growth curve for inferior vena caval diameter in healthy pediatric patients: brief report of initial curve development, Crit Ultrasound J., 2012, 4, 1, 12

[11] Juhl-Olsen, P., Vistisen, ST., Christiansen, L.K., Rasmussen, L.A., Frederiksen, C.A., Sloth, E., Ultrasound of The Inferior Vena Cava Does Not Predict Hemodynamic Response To Early Hemorrhage, J Emer Med., 2013, 45, 4, 592-597

[12] Kimura, BJ., Dalugdugan, R., Gilcrease, GW., Phan, JN., Showalter, B.K., Wolfson, T., The effect of breathing manner on inferior vena caval diameter, Eur J Echocard, 2011, 12, 120-123

[13] Kircher, B.J., Himelman, R.B., Schiller, N.B., Noninvasive estimation of right atrial pressure from the inspiratory collapse of the inferior vena cava, Am J Cardiol, 1990, 66, 4, 493-496

[14] Kitamura, H., Kobayashi, C., Impairment of change in diameter of the hepatic portion of the inferior vena cava: a sonographic sign of liver fibrosis or cirrhosis, J Ultrasound Med., 2005, 24, 3, 355-359

[15] Krupa, A., Fichtinger, G., Hager, G.D., Full Motion Tracking in Ultrasound Using Image Speckle Information and Visual Servoin, Proc. ICRA, 2007, 2458-2464

[16] Lyon, M., Blaivas, M., Brannam, L., Sonographic measurement of the inferior vena cava as a marker of blood loss, Am J Emerg Med, 2005, 23, 1, 45-50

[17] Moreno, F.L., Hagan, A.D., Holmen, J.R., Pryor, T.A., Strickland, R.D., Castle, C.H., Evaluation of size and dynamics of the inferior vena cava as an index of right-sided cardiac function, 1984, Am J Cardiol, 53, 4, 579-585

[18] Nakamura, K., Tomida, M.,,o, T., Sen, K., Inokuchi, R., Kobayashi, E., Nakajima, S., Sakuma, I., Yahagi, N., Cardiac variation of inferior vena cava: new concept in the evaluation of intravascular blood volume, J Med Ultrasonics, 2013, 40, 205-209

[19] Pirat, B., Khoury, D.S., Hartley, C.J., Tiller, L., Rao, L., Schulz, D.G., Nagueh, S.F., Zoghbi, W.A., A Novel Feature Tracking Echocardiographic Method for the Quantitation of Regional Myocardial Function: Validation in an Animal Model of Ischemia-Reperfusion, J Am Coll Cardiol., 2008, 51, 6, 651-659

[20] Resnick, J., Cydulka, R., Platz, E., Jones, R., Ultrasound Does Not Detect Early Blood Loss In Healthy Volunteers Donating Blood, J Emer Med., 2011, 41, 3, 270-275

[21] Wallace, DJ., Allison, M., Stone, M.B., Inferior vena cava percentage collapse during respiration is affected by the sampling location: an ultrasound study in healthy volunteers, Acad Emerg Med, 2010, 17, 1, 96-99

[22] Weekes, A.J., Lewis, M.R., Kahler, Z.P., Stader, D.E., Quirke, D.P., Norton, H.J., Almond, C., Middleton, D., Tayal, VS., The effect of weight-based volume loading on the inferior vena cava in fasting subjects: a prospective randomized double-blinded trial, Acad Emerg Med., 2012, 19, 8, 901-907

[23] Yang, L., Georgescu, B., Zheng, Y., Meer, P., Comaniciu, P., 3D Ultrasound Tracking of the Left Ventricles Using One-Step Forward Prediction and Data Fusion of Collaborative Trackers, Proc. IEEE Conf Comput Vis Pattern Recognit, 2008

[24] Yeung, F., Levinson, S.F., Fu, D., Parker, K.J., Feature-Adaptive Motion Tracking of Ultrasound Image Sequences Using A Deformable Mesh, IEEE Trans. Med. Imaging, 1998, 17, 6, 945-956

[25] Zhang, Z., Xu, X., Ye, S., Xu, L., Ultrasonographic Measurement of the Respiratory Variation in the Inferior Vena Cava Diameter Is Predictive of Fluid Responsiveness in Critically Ill Patients: Systematic Review and Meta-analysis, Ultrasound Med Biol, 2014, in press